Accepted to ApJ

Cataclysmic and Close Binaries in Star Clusters. V. Erupting Dwarf Novae, Faint Blue Stars, X-ray sources, and the Classical Nova in the Core of M80[1]

Michael M. Shara

Department of Astrophysics, American Museum of Natural History, 79th St. and Central Park West, New York, NY, 10024

mshara@amnh.org

Sasha Hinkley

Department of Astrophysics, American Museum of Natural History, 79th St. and Central Park West, New York, NY, 10024

shinkley@amnh.org

David R. Zurek

Department of Astrophysics, American Museum of Natural History, 79th St. and Central Park West, New York, NY, 10024

dzurek@amnh.org

ABSTRACT

Large populations of cataclysmic variables (CVs) in globular clusters have long been predicted, but the number of absolutely certain cluster CVs known in globulars is still less than 10. HST and Chandra observers have recently found dozens of cataclysmic variable candidates in several populous globular clusters. Confirmation and characterization of these candidates are extremely difficult, thus identification of unambiguous CVs remains important. We have searched

[1]Based on observations with the NASA/ESA *Hubble Space Telescope*, obtained from the Data Archive at the Space Telescope Science Institute,which is operated by the Association of Universities for Research in Astronomy, Inc., under NASA contract NAS5-26555. These observations are associated with program #6460.

all archival HST images of the dense globular cluster M80 for erupting dwarf novae (DN), and to check the outburst behaviors of two very blue objects first identified a decade ago. Two new erupting dwarf novae were found in 8 searched epochs, making M80 a record holder for erupting DN. The quiescent classical nova in M80 varies by no more than a few tenths of a magnitude on timescales of minutes to years, and a similar faint, blue object varies by a similar amount. Simulations and completeness tests indicate that there are at most 3 erupting DN like SS Cyg and at most 9 U Gem-like DN in M80. Either this very dense cluster contains about an order of magnitude fewer CVs than theory predicts, or most M80 CVs are extremely faint and/or erupt very infrequently like WZ Sge. We have detected a sequence of 54 objects running parallel to the main sequence and several tenths of a magnitude bluewards of it. These blue objects are significantly more centrally concentrated than the main sequence stars, but not as centrally concentrated as the blue stragglers. We suggest that these objects are white dwarf–red dwarf binaries, and that some are the faint CV population of M80.

Subject headings: Stars: Cataclysmic Variables— dwarf novae, galaxies: individual (LMC)

1. Introduction

The discovery of unexpectedly rich populations of luminous X-ray sources in Galactic globular clusters (Clark 1975; Katz 1975) was a sharp challenge to theorists. Efficient mechanisms for generating large numbers of mass-transferring binaries, dominated by a compact primary, were required to explain the observations. Tidal capture scenarios involving two stars (Fabian, Pringle, & Rees 1975) and/or exchange reactions involving three stars (Hills 1976) were rapidly developed. These processes are now believed to be the sources of the neutron star-dominated X-ray binaries in globular clusters. Strong observational evidence in favor of these scenarios is the remarkable correlation between stellar encounter rate and number of X-ray sources in globular cluster cores (Pooley et al. 2003).

These two and three-body mechanisms also predict large populations (Di Stefano & Rappaport 1994) of accreting white dwarf-main sequence star binaries—the cataclysmic variable (CV) stars. Unfortunately only one globular cluster dwarf nova (DN) is easily resolved and studied from the ground: V101 in M5 (Margon, Downes & Gunn 1981), (Shara, Potter, & Moffat 1990), (Neill, Shara, Caulet, & Buckley 2002). The large amplitude variations of many CVs (Warner 1995) suggest that Hubble Space Telescope (HST) observations of globular clusters would easily locate dozens in the core of each cluster. With expected apparent

magnitudes in the range 17-23, prototypical CVs like SS Cyg and U Gem should be trivial to find. It would clearly be of enormous benefit to CV science if dozens of these objects, all at the same distance and with the same parent metallicity, could be located. Accurate luminosity functions, and bias-free period distributions and eruption frequencies could be derived to confront theoretical models. Tidal capture CVs could be contrasted with those produced by ordinary binary evolution. Systematic variations in outburst properties and orbital distributions might be uncovered.

Remarkably, only a handful of absolutely certain CVs in globular clusters are known today. These include a few dwarf novae seen in eruption (e.g. (Paresce & De Marchi 1994), (Charles, Clarkson, & van Zyl 2002), (Anderson, Cool, & King 2003)), one classical nova (Auwers 1886), (Shara & Drissen 1995), and a few spectrographically confirmed, very blue faint stars (e.g. (Grindlay et al. 1995), (Deutsch, Margon, Anderson, & Downes 1999; Knigge et al. 2003)). Recently, dozens of CV candidates have been identified in 47 Tuc (Grindlay, Heinke, Edmonds, & Murray 2001), (Knigge, Zurek, Shara, & Long 2002), M80 (Heinke et al. 2003) and in NGC 6397 (Grindlay et al. 2001) through deep Chandra X-ray Observatory and HST observations. Unfortunately, large amounts of HST and Chandra time are essential for follow-up studies, so unambiguous characterization of all candidates may take many years. Thus any new, unambiguous CVs that can be found in archival data are well worth searching for.

About half of all known field CVs (Downes et al. 2001) are dwarf novae (DN). Most known DN reveal themselves through 2-5 magnitude outbursts every few weeks to months (Warner 1995); similar DN in clusters should be identifiable in multi-epoch images. Since large archival HST datasets of globulars are available we have been systematically looking for erupting dwarf novae in the cores of all such clusters. Here we report the results of an extensive and successful search of M80.

M80 is one of the densest globular clusters in the Milky Way, with a spectacular blue straggler sequence (Ferraro et al. 1999), a quiescent old nova (Shara & Drissen 1995), and 19 X-ray sources (Heinke et al. 2003). A detailed comparison of M80 with 47 Tuc (Heinke et al. 2003) suggests that the encounter rate in M80 is about a factor of two lower; roughly 50 CVs should exist in M80 as of order 100 are predicted in 47 Tuc (Di Stefano & Rappaport 1994).

In section 2 we present the observational database, search strategy, and the photometry of variables. The erupting DN, non-eruptive CV candidates and their light curves are shown in section 3. We discuss whether the candidates could be other kinds of variables in section 4. In section 5 we report simulations to test our completeness, and to place limits on the numbers of DN of various luminosities in M80. We report on a remarkable sequence of very

blue, centrally located objects in section 6, and our attempts to match these with the M80 X-ray sources in section 7. We briefly summarize our results in section 7.

2. Observations

The Hubble Space Telescope has imaged M80 during 8 separate epochs from 1994 to 2000. All epochs except the last included F336W frames, particularly useful in detecting blue objects. The pass-band of the F450W frames of the last epoch is close to the F439W passband of epochs 1 and 2, so that essentially constant limiting magnitude is attained for our 8 epoch survey (see section 5). The dates of observation, PI of program and program number, filters used, number of frames and total exposure time in each filter are given in the observing log which is Table 1.

The individual WFPC2 images were combined using the "Montage2" routine contained within the stand-alone DAOphot package. These frames were run through DAOphot's matching program "DAOmaster" to derive the subpixel frame-to-frame shifts and thereby register all images to the first image of the first epoch. These shifts were passed to Montage2, which produced a single, sky subtracted, high signal-to-noise image for each epoch and filter. HST was not perfectly aligned at all epochs in all filters. Figure 1 is an overview of the fields of view of the 8 epochs, with four of the most interesting objects that we found (section 3) indicated.

The dwarf-nova candidates (Figure 2) were found by image differencing *and* by blinking rapidly through groups of the F336W frames to look for any subtle changes in the appearance of the stellar field. Dwarf novae should rise from invisibility to easily detectable in the timeframe defined by the observations. Brightening from previously empty regions of the sky is easily seen.

In order to detect extremely faint stars, a master list of stars was derived using the technique of Richer et al. (2004). This technique rejects the brigher pixels from a stack, giving emphasis to fainter pixels, and thus probing deeper. In addition, point spread functions were created for the F336W, F450W, F656N, and F675W (U, B, $H\alpha$ and R) data and then provided to the allframe software (Stetson 1994) for multi-image simultaneous PSF fitting to derive positions and magnitudes for as many stars as possible. The photometry was then converted to the ST magnitude system as described in Shara & Drissen (1995). The resulting color-magnitude diagram (CMD) of M80, the deepest ever produced, is shown in Figures 3 and 4. The two new dwarf nova candidates are evident, as are the two very blue stars first noted by Shara & Drissen (1995). In addition, many more faint blue objects—about 50 in

all—are now visible in this deeper CMD. Some of these very blue objects are also indicated in the finder chart that is Figure 5, and discussed in sections 6 and 7.

3. Dwarf Novae and the Classical Nova

To be recognized as a candidate, a variable had to be visible on all frames in at least one of the eight epochs, and to have varied by more than 1.0 magnitudes between its faintest and brightest state. This selection method revealed two dwarf nova candidates from the entire dataset (and no other obvious variables). These two strongly varying, very blue candidates which we label DN1 and DN2 are erupting in epochs 3 and 6, respectively. Their positions are: for DN1 $\alpha(2000) = 16{:}17{:}02.2$, $\delta(2000) =$ -22:58:37.9; and for DN2, $\alpha(2000) =$16:16:59.8, $\delta(2000) =$ -22:58:18.0. The nightly images of these two objects are shown in Figures 6 and 7, and their photometry is presented in Figures 8 and 9. We defer a discussion of these stars and their implications until after the next section, where we simulate expected DN images and light curves.

We show the images and photometry of the likely quiescent old nova (T Sco 1860 A.D.) in Figures 10 and 11, respectively. Brightness fluctuations do not exceed a few tenths of a magnitude. The mean apparent F336W magnitude is 21.5, corresponding to an absolute U-band magnitude of 6.5, well within the range of old nova luminosities (Warner 1995).

Finally, we show in Figures 12 and 13 the images and lightcurve of the faint blue object noted by Shara & Drissen (1995). Located close to T Sco in the M80 color-magnitude diagram, it too varies by at most a few tenths of a magnitude. Whereas the T Sco lightcurve shows several points in a given epoch, the faint blue object's lightcurve shows only one brightness value for each epoch. The object lies rather close to the HST Planetary Camera (PC) chip's edge, and photometry was performed on the individual-epoch, CR-rejected images to boost the signal-to-noise. While its brightness and color are very suggestive, this object remains a CV candidate, and not a confirmed CV, until it is eventually shown to erupt as a DN or found to have a spectrum consistent with cataclysmic classification.

4. Simulations of Known Dwarf Novae

To estimate our detection completeness for erupting dwarf novae to various magnitude limits we carried out simulations of eruptions for two of the best known and characterized Galactic dwarf novae: SS Cyg, and U Gem. (These objects have accurately determined parallaxes (Harrison et al. 1999) and, using their well tabulated apparent magnitudes (Warner

1995), the absolute magnitudes are easily calculated. These two dwarf novae were chosen to represent, respectively, the most luminous and more typical values of absolute magnitudes seen for erupting and quiescent DN). To simulate SS Cyg, 100 artificial PSFs were placed in random positions across an M80 HST F336W image of a single epoch. For these 100 PSFs, brightnesses were determined by picking 100 random points from the SS Cyg American Association of Variable Star Observers (AAVSO) lightcurve stretching over 1000 days. These 100 artificial dwarf novae, (now mimicking SS Cyg at 100 random places in its lightcurve), were shifted to the apparent magnitudes they would have at the 10.3 kpc distance of M80 (Brocato et al. 1998). This image was then blinked against an image (at a different epoch) with these same artificial PSFs corresponding to SS Cyg in quiescence. The same procedure was performed for U Gem, using 100 randomly sampled brightnesses from 1000 days of the U Gem lightcurve. Typical images of these simulated dwarf novae, each at their maximum, intermediate and minimum brightness, are shown in Figure 14. Our simulations show that, by comparing two randomly selected epochs, one detects an SS Cygni-like dwarf nova $25.0 \pm 3.3\%$ of the time, while U Gem is detected $6.0 \pm 1.7\%$ of the time. The detection probability is thus $P_{SS} = 0.125$ per epoch for SS Cyg and $P_{UG} = 0.030$ for U Gem. In each independent epoch, we therefore expect that the probability of *not seeing* a given SS Cyg in eruption is $1 - 0.125 = 0.875$, and the probability of not seeing a given U Gem in eruption is $1 - 0.030 = 0.970$. Thus in eight independent epochs (a more pessimistic case than our own 8 epochs, where 5 epochs are precisely at weekly intervals) we might expect to not see SS Cyg $(0.875)^8 = 34\%$ of the time, and we expect to miss U Gem-like objects $(0.97)^8 = 78\%$ of the time. Equivalently, we expect to see at least $1 - 0.34 = 66\%$ of SS Cyg-like eruptions and at least $1 - 0.78 = 22\%$ of all U Gem-like eruptions.

5. Interpretation

5.1. Have We Found Erupting M80 Dwarf Novae?

Comparison of the two erupting DN candidates shown in Figures 6 and 7 with the M80-DN simulation images shown in Figure 14 demonstrates that the brightness and variability behaviors of our candidates are consistent with those expected of moderately luminous erupting dwarf novae in M80. All erupting dwarf novae achieve outburst U band absolute magnitudes $\lesssim 5$, and the simulations of Figure 15 show that we easily reached fainter than that limit in all epochs. The very blue outburst colors, outburst brightnesses, presence and blue colors in quiescence, our completeness of detection of stars at different magnitudes (Figure 15), and strong concentration to the center of M80 all argue very strongly in favor of DN1 and DN2 being dwarf novae. However, in the absence of spectra or a second recorded

outburst, one could always argue that one or both of these are variables of some other type, perhaps not even associated with M80.

What are possible variables that might mimic M80 DN behavior? Amongst these are: chance superpositions of background supernovae or classical novae, gamma ray bursts (GRB), microlensing events or Milky Way variables along the line of sight to M80. Large area, multi-epoch surveys for faint variables (e.g. Hawkins (1984)) show that the strong central concentration of our variables to the core of M80 (and the moderately high galactic latitude of the cluster, 19.5°) is far too high for them to be field RR Lyrae stars or supernovae.

The brightness and very blue colors of the candidates rule out other types of Galactic variables. RR Lyrae and flare stars don't match the observed brightness and/or blue colors of the two DN candidates. The rarity of GRB (about 1 over the entire sky per day) and microlensing events, and the very blue colors of our variables almost certainly rules out these possibilities. But while the magnitudes and colors both during outburst and quiescence of our DN candidates argue strongly for that classification, an absolutely certain characterization will require challenging but important follow-up observations. These include

1) Spectra near quiescence (to demonstrate the presence of Balmer emission lines).

2) Imagery every day or two for several months with HST to reveal repeated eruptions separated by weeks to months.

3) Several hours of HST time-resolved UV or optical photometry to reveal the orbital modulation characteristic of CVs.

5.2. Detections versus Expected Detections

The size of our field of view was 1574 arcsec^2, extending out to 1.9 core radii from the cluster center. The average time between eruptions for 21 well studied Galactic DN is 29 days (Szkody & Mattei 1984). The length and depth of our observing run (5 epochs spaced 1 week apart, and three other random epochs) taken by themselves suggest that most erupting SS Cyg-like or U Gem-like dwarf nova would have been detected. In fact, our simulations of SS Cyg and especially of U Gem (in section 4) demonstrate that outburst frequency is the key parameter in determining whether a given dwarf nova will be detected. SS Cyg is intrinsically more luminous in outburst than U Gem, but both are straightforward to detect, in eruption, in our dataset. It is the relative infrequency of U Gem outbursts that makes it three times less likely (22%) to be detected than SS Cyg-like outbursts. Given these probabilities of detecting SS Cyg and U Gem-like dwarf nova eruptions in M80, what limits

can we place on the total populations of similar objects in the cluster? Since we have only seen 1 eruption of each of the M80 DN we don't know their eruption frequency or maximum luminosity. Either could be U Gem-like or SS Cyg-like. Our conservative estimate is that there are $\lesssim 2/0.66 = 3$ SS Cyg-like DN in M80, and $\lesssim 2/0.22 \sim 9$ U Gem-like DN in the cluster.

The fact that we detected only two erupting DN, and that there are almost certainly fewer than ~ 9 DN in M80, when (the admittedly simple) tidal capture model predicts an order of magnitude more CVs suggests that

i) SS Cyg and U Gem-like CVs in M80 are $\sim 50/9 \sim 6\times$ fewer in number than theory predicts, and/or

ii) most CVs are more like the rarely erupting WZ Sge, and much fainter than the prototypical DN SS Cyg and U Gem, and/or

iii) globular CVs may be mostly magnetic (Grindlay et al. 1995)and non-eruptive.

What is the true, average inter-outburst period for all dwarf novae? Unfortunately, the answer is unknown. CV catalogs are dominated by the easy-to-find, frequently outbursting DN. In addition, the distances to all but a dozen or so Galactic DN are too uncertain to yield an accurate luminosity distribution. (We note that the canonical literature distance to the prototypical DN, SS Cyg, was in error by a factor of two until HST parallaxes became available in 2000). A warning that CV populations may be dominated by extremely faint and/or infrequently erupting DN is personified in the nearest known DN, WZ Sge. This object is a mere 43.5 pc away (Thorstensen 2003), (Harrison et al. 2004) with absolute visual magnitudes at minimum and maximum of 11.8 and 3.9, and 1–2 month-long eruptions separated by about 25 years. Our chances of detecting a WZ Sge-like outburst are two orders of magnitude smaller than the likelihood of detecting a U Gem-like eruption (again, because of the relative outburst frequency). There could easily be 100 WZ Sge stars in M80—and our chances of detecting even one in our dataset would only be of order 20%. We conclude that: there are ~ 3 or fewer SS Cyg-like, or 9 or fewer U Gem-like DN in M80. However, 100 WZ Sges could exist in the cluster. If most CVs are similar to WZ Sge (often referred to as CV "graveyard" objects) then the small number of detected M80 DN is naturally explained.

6. The Faint Blue Objects in M80

The deep U vs. $(U-B)$ CMD of Figure 5 contains a remarkable sequence of 54 objects running parallel to the main sequence and between 0.3 and 1.4 magnitudes blueward of it.

We have verified that these faint blue objects are not due to e.g. "hot" pixels by comparing their images on frames from different epochs with significant spatial offsets. While it is certainly possible that some of these objects' blue colors are due to photometric errors, at least a dozen objects with $(U-B) < 0.1$ are (on visual inspection) very blue and unblended. This is precisely the part of the CMD that would be occupied by CVs and non-interacting white dwarf-red dwarf binaries. If these 54 objects are, indeed CVs and/or WD-RD binaries then they must possess masses larger than main sequence stars of similar magnitude. Equipartition of energy should then have concentrated these blue objects towards the cluster center. This, in fact, is an acid test that must be passed if we are to give credence to the suggestion of the blue M80 stars as a WD-RD binary sequence. Figure 16 strongly suggests that these blue stars are more centrally concentrated than main sequence stars, at least at $r > 8$ arcsec from the cluster center. The K-S test determines that the blue objects and main sequence stars of Figure 16 do not share the same radial distribution with $> 95\%$ confidence. The blue stragglers and main sequence stars are even more dramatically separated in Figure 16. The K-S test states that the BS and MS stars are drawn from different radial distributions with $> 99.5\%$ likelihood.

Artificial star tests were performed to determine the the recovery rate for artificial stars placed randomly on the chip. Figure 17 shows the fraction of stars recovered in 8 different annuli centered on the center of the cluster, for several different brightesses. These simulations show that we approach maximum completeness ($\sim 80\%$) for the fainter blue stars with $U > 22$ only when $r > 8$ arcsec from the core of M80. *Thus the apparent weak central concentration of the blue stars in the inner 8 arcsec is probably due to significant incompleteness of the sample of these very faint objects in the core of the cluster, rather than their physical absence.*

The central concentration of blue stragglers in globular clusters is ubiquitous and well established for many clusters e.g. (Paresce et al. 1991; Ferraro et al. 1999), and indicative of objects with measured masses 2-3 times the turnoff mass (Shara, Saffer, & Livio 1997; Saffer et al. 2002). We conclude from Figure 16 that the blue sequence stars of Figure 13 are intermediate in mass between the main sequence and blue straggler stars —exactly as one expects for WD-RD binaries.

7. X-ray sources and Faint Blue Objects

We have compared the positions of our four objects of interest (DN1, DN2, T Sco and the Shara-Drissen object) as well as the 54 faint, blue objects with the 19 X-ray sources noted by Heinke et al. (2003). The Right Ascension and Declinations of our full sample of 58 CVs

and CV candidates were offset in an iterative manner until we found the optimal minimum separation between the 19 X-ray sources and the CV candidates. The best overall match (in the least-squares sense) occurs with offsets of $\Delta\alpha \simeq -0.5''$ and $\Delta\delta \simeq +4.7''$ applied to the CV candidates, with or without the two significant outliers CX10 and CX19 removed. The resulting source distributions are shown in Figure 18. The 19 X-ray source positions together with the adjusted positions of the closest faint blue stars are listed in Table 2.

The nearly 5" offset between the 19 X-ray sources and the 58 CVs and CV candidates is much larger than the uncertainties in HST and Chandra pointings. We also find no correlation between the 19 X-ray sources' luminosities and the F336W brightnesses of the 19 "matched" faint blue stars in Table 2. We interpret this to mean that, while the two populations are centrally concentrated, many (and probably most or all) of the apparent matches of Table 2 are spurious. Deep HST far-UV observations of M80 are currently being scheduled, and these will be important for providing optical-UV counterparts to this cluster's X-ray sources.

Finally, we have also checked the Hα luminosities of the 54 faint blue sources. An R versus H$\alpha - R$ color-magnitude diagram is shown in Figure 19. Of the full sample of 54 blue objects, 51 had measurable Hα fluxes. None of these faint blue sources appear to have an Hα brightness more significant than that of the overall cluster population. If these are degenerate star–red dwarf binaries then their mass transfer rates are very low or zero.

8. Conclusions

We have observed M80 during 8 separate epochs with sufficient resolution and sensitivity to detect any erupting dwarf novae within the inner 1.9 core radii of that cluster. Two very strong candidates, with outburst colors, brightnesses, central concentration, and presence in quiescence, all consistent with DN classification, were detected. The old nova candidate T Sco (nova 1860) and another very blue, faint star (Shara & Drissen 1995) are remarkably constant in brightness. Simulations and completeness tests indicate that ≤ 3 regularly outbursting dwarf novae similar to SS Cyg, and $\lesssim 9$ U Gem-like dwarf novae exist today in M80. The presence of several dozen very faint blue, centrally concentrated stars in the core of M80 hints at a large red dwarf–degenerate star binary population; some of these may be a very rarely-erupting CV population.

We acknowledge with thanks the variable star observations from the AAVSO International Database contributed by observers worldwide and used in this research.

Support for program #6460 was provided by NASA through a grant from the Space Telescope Science Institute, which is operated by the Association of Universities for Research in Astronomy, Inc., under NASA contract NAS 5-26555."

REFERENCES

Anderson, J., Cool, A. M., & King, I. R. 2003, ApJ, 597, L137

Auwers, A. 1886, Astronomische Nachrichten, 114, 47

Bailey, J. 1980, MNRAS, 190, 119

Brocato, E., Castellani, V., Scotti, G. A., Saviane, I., Piotto, G., & Ferraro, F. R. 1998, A&A, 335, 929

Bruch, A. & Engel, A. 1994, A&AS, 104, 79

Charles, P. A., Clarkson, W. I., & van Zyl, L. 2002, New Astronomy, 7, 21

Clark, G. W. 1975, ApJ, 199, L143

Deutsch, E. W., Margon, B., Anderson, S. F., & Downes, R. A. 1999, AJ, 118, 2888

Di Stefano, R. & Rappaport, S. 1994, ApJ, 423, 274

Downes, R. A., Webbink, R. F., Shara, M. M., Ritter, H., Kolb, U., & Duerbeck, H. W. 2001, PASP, 113, 764

Fabian, A. C., Pringle, J. E., & Rees, M. J. 1975, MNRAS, 172, 15P

Ferraro, F. R., Paltrinieri, B., Rood, R. T., & Dorman, B. 1999, ApJ, 522, 983

Grindlay, J. E., Cool, A. M., Callanan, P. J., Bailyn, C. D., Cohn, H. N., & Lugger, P. M. 1995, ApJ, 455, L47

Grindlay, J. E., Heinke, C., Edmonds, P. D., & Murray, S. S. 2001, Science, 292, 2290

Grindlay, J. E., Heinke, C. O., Edmonds, P. D., Murray, S. S., & Cool, A. M. 2001, ApJ, 563, L53

Harrison, T. E., McNamara, B. J., Szkody, P., McArthur, B. E., Benedict, G. F., Klemola, A. R., & Gilliland, R. L. 1999, ApJ, 515, L93

Harrison, T. E., Johnson, J. J., McArthur, B. E., Benedict, G. F., Szkody, P., Howell, S. B., & Gelino, D. M. 2004, AJ, 127, 460

Hawkins, M. R. S. 1984, MNRAS, 206, 433

Heinke, C. O., Grindlay, J. E., Edmonds, P. D., Lloyd, D. A., Murray, S. S., Cohn, H. N., & Lugger, P. M. 2003, ApJ, 598, 516

Hills, J. G. 1976, MNRAS, 175, 1P

Hills, J. G. & Day, C. A. 1976, Astrophys. Lett., 17, 87

Katz, J. I. 1975, Nature, 253, 698

Knigge, C., Zurek, D. R., Shara, M. M., & Long, K. S. 2002, ApJ, 579, 752

Knigge, C., Zurek, D. R., Shara, M. M., Long, K. S., & Gilliland, R. L. 2003, ApJ, 599, 1320

Margon, B., Downes, R.A., & Gunn, J. E. 1981, ApJ, 247, L89

Neill, J. D., Shara, M. M., Caulet, A., & Buckley, D. A. H. 2002, AJ, 123, 3298

Paresce, F., Meylan, G., Shara, M., Baxter, D., & Greenfield, P. 1991, Nature, 352, 297

Paresce, F. & de Marchi, G. 1994, ApJ, 427, L33

Pogson, N. 1860, MNRAS, 21, 32

Pooley, D., et al. 2003, ApJ, 591, L131

Pryor, C. & Meylan, G. 1993, ASP Conf. Ser. 50: Structure and Dynamics of Globular Clusters, 357

Richer, H. B., et al. 2004, AJ, 127, 2904

Saffer, R. A., Sepinski, J. F., Demarchi, G., Livio, M., Paresce, F., Shara, M. M., & Zurek, D. 2002, ASP Conf. Ser. 263: Stellar Collisions, Mergers and their Consequences, 157

Shara, M. M., Potter, M., & Moffat, A. F. J. 1990, AJ, 100, 540

Shara, M. M. & Drissen, L. 1995, ApJ, 448, 203

Shara, M. M., Saffer, R. A., & Livio, M. 1997, ApJ, 489, L59

Shara, M. M., Zurek, D. R., Baltz, E. A., Lauer, T. R., & Silk, J. 2004, ApJ, 605, L117

Stetson, P. B. 1994, PASP, 106, 250

Stetson, P. B. 2000, PASP, 112, 925

Szkody, P. & Mattei, J. A. 1984, PASP, 96, 988

Thorstensen, J. R. 2003, AJ, 126, 3017

Tody, D. 1986, Proc. SPIE, 627, 733

Verbunt, F. & Hut, P. 1987, IAU Symp. 125: The Origin and Evolution of Neutron Stars, 125, 187

Warner, B. 1995, Cambridge Astrophysics Series, Cambridge, New York: Cambridge University Press, —c1995,

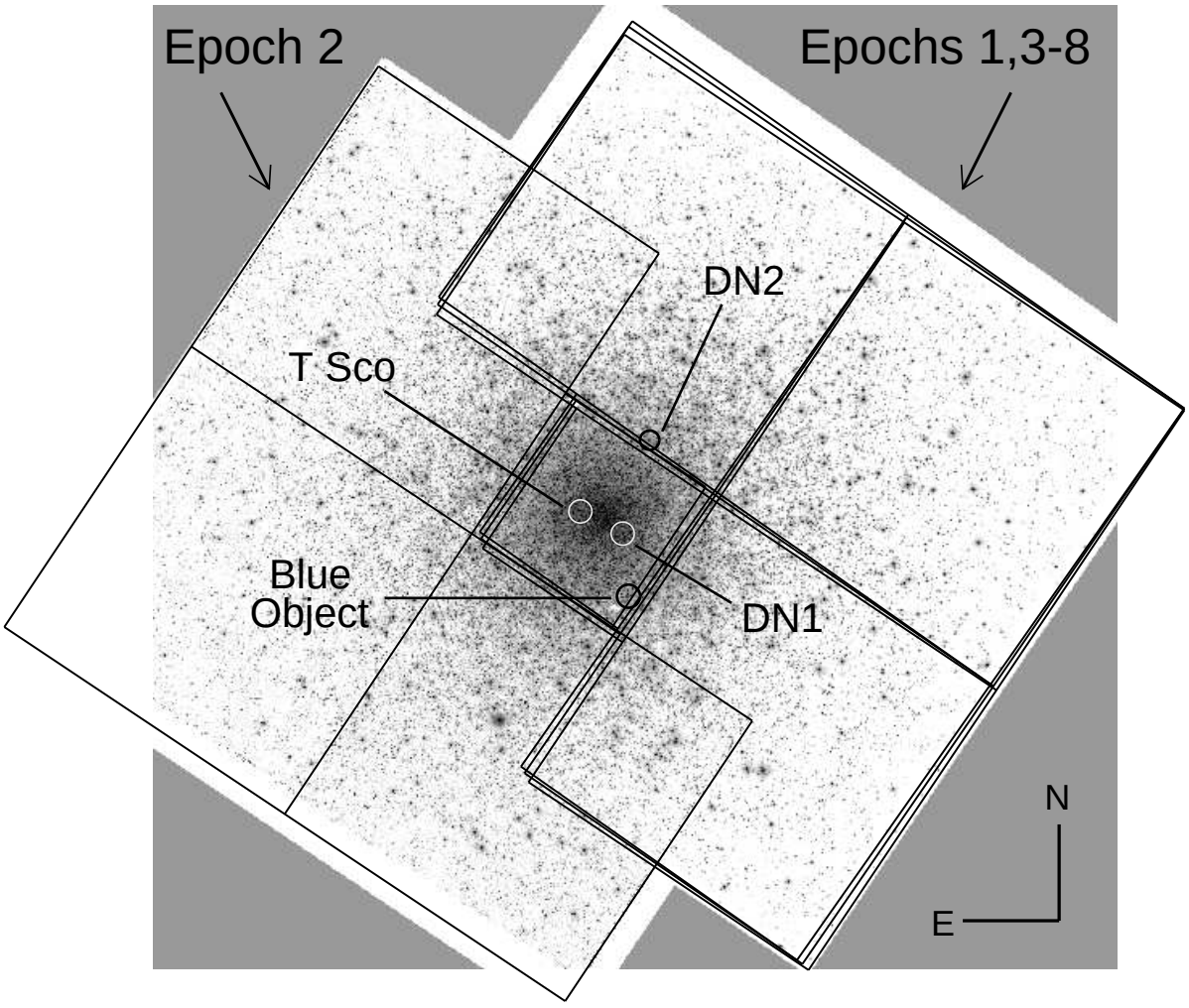

Fig. 1.— A mosaic of HST images of the field of M80, indicating the orientations of our 8 epochs of observation.

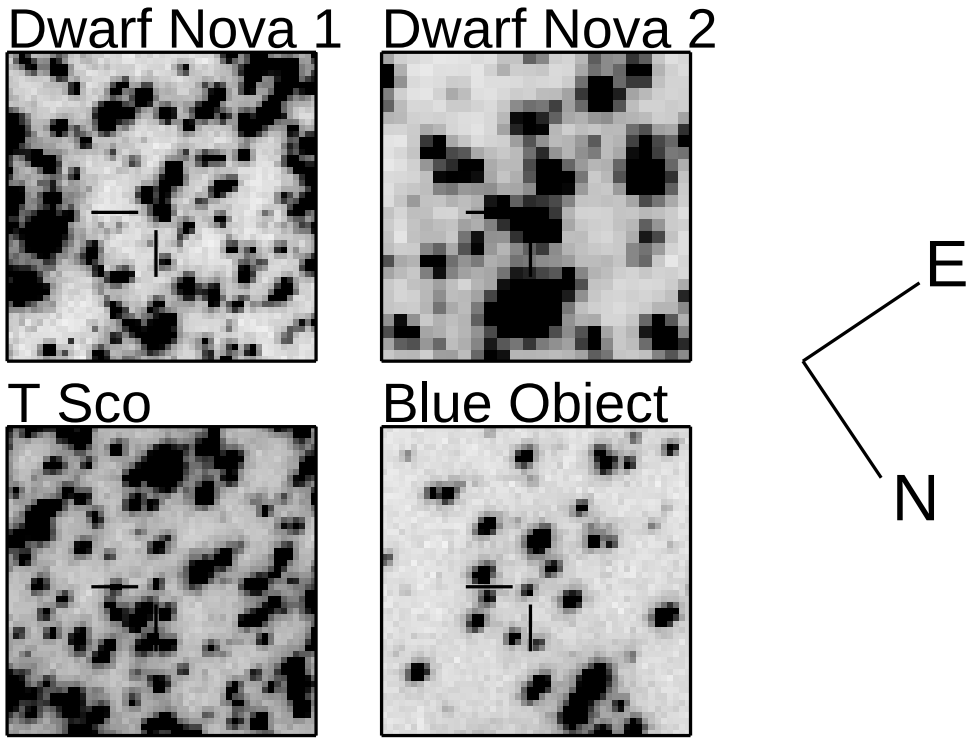

Fig. 2.— A closer view of each of the four objects of interest. Each image is 2.37 arcseconds on a side. The lower resolution in the image of Dwarf Nova 2 reflects the fact that this object was only imaged on the HST WF4 chip, while all the others were imaged on the higher resolution Planetary Camera CCD.

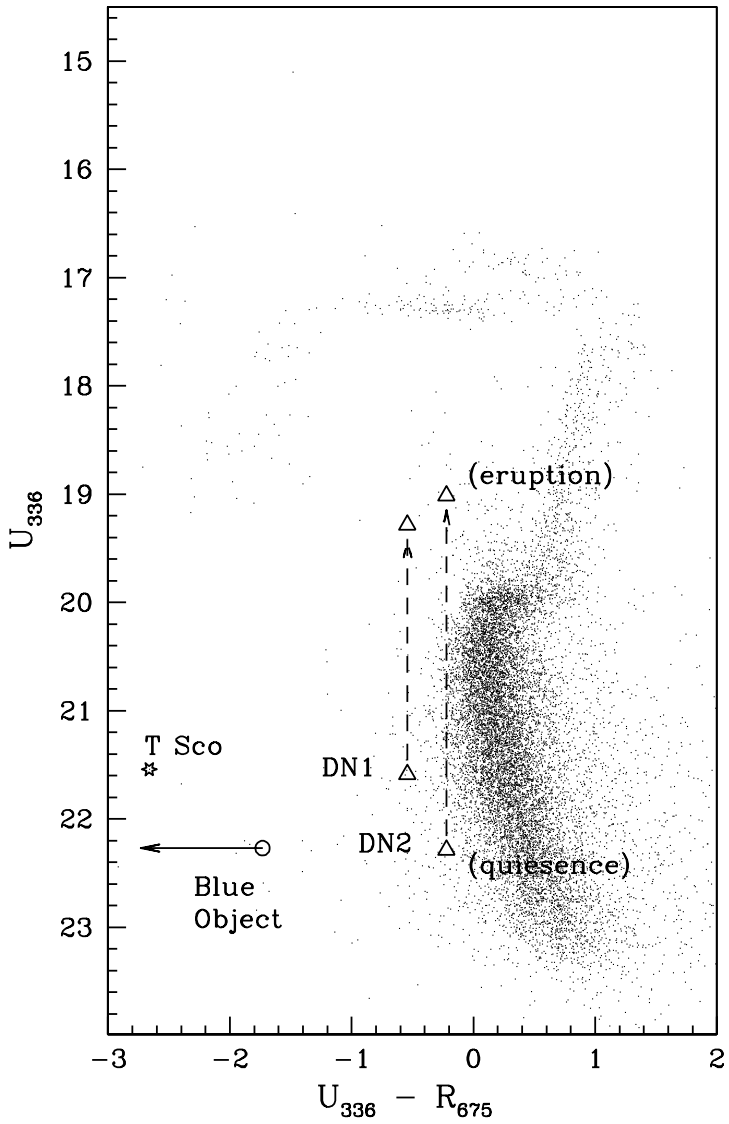

Fig. 3.— CMD for M80. In the plot, the four objects of Figure 1 are marked. Since there was only R imaging for one epoch (epoch 3), obtaining both eruption and quiescent *colors* was impossible. The range of U magnitudes for the two dwarf novae are shown to give a sense of the overall range during outburst. In addition, since the Blue Object was essentially invisible in the R-band, an R value near the plate limit was assumed, hence the upper limit arrow indicated.

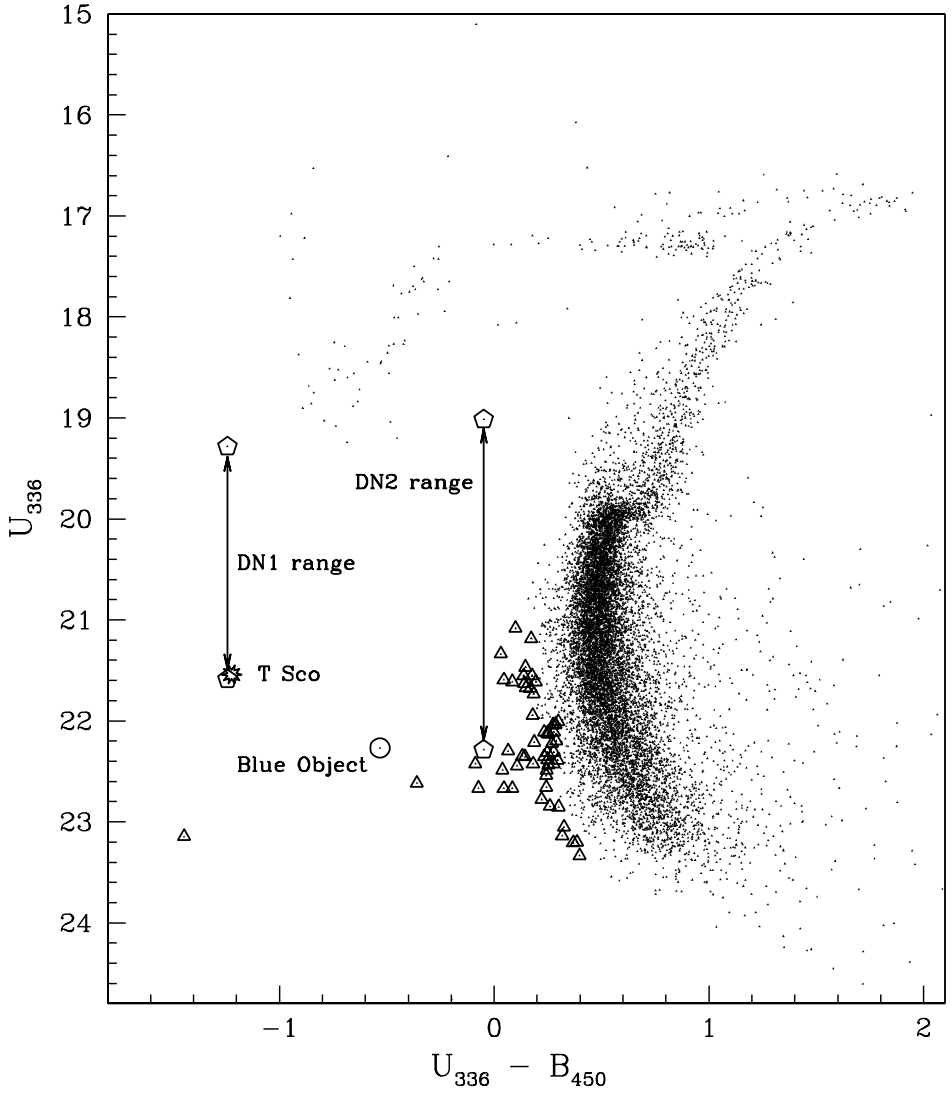

Fig. 4.— The U versus $(U-B)$ CMD for M80. The 54 triangles that lie blueward of the main sequence are newly detected white dwarf-red dwarf binary and/or CV candidates. The four objects discussed in this paper are also marked. The faint blue object of Shara & Drissen (1995) is marked with a circle, while T Sco (nova 1860) is starred. Note that the location of T Sco is nearly coincident with the first dwarf nova (DN1) in its quiescent state. As before, the brightness ranges of the two dwarf novae DN1 and DN2 are marked.

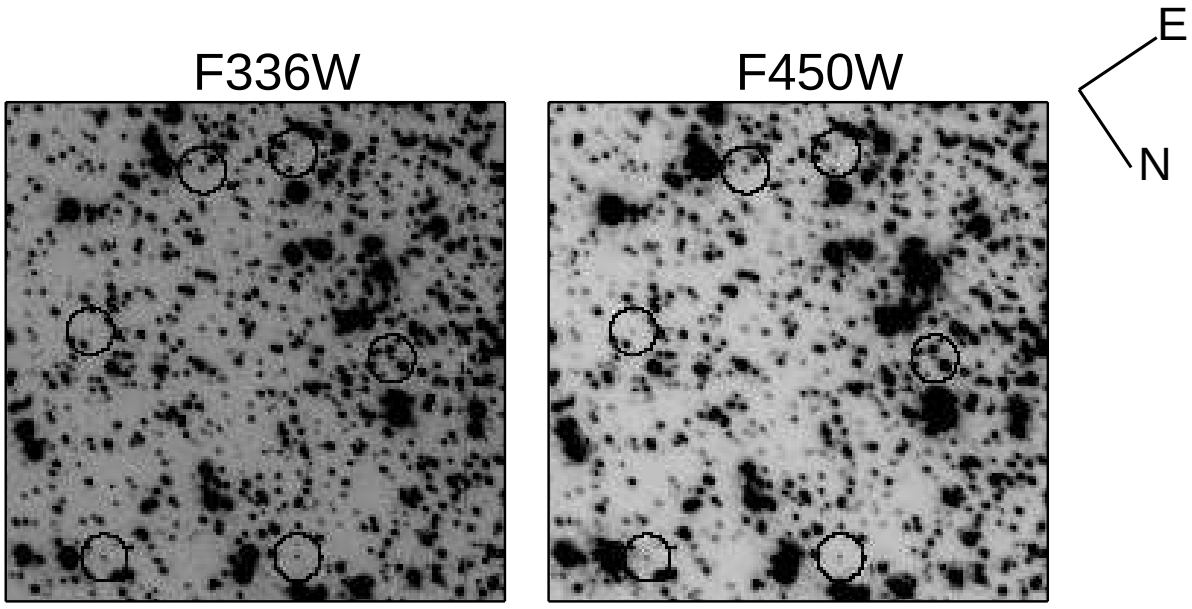

Fig. 5.— Two subregions of the F336W and F450W PC images showing a handful of those objects significantly more blue than the main sequence. North and East are as indicated. Each image is 8.38 arcseconds on a side.

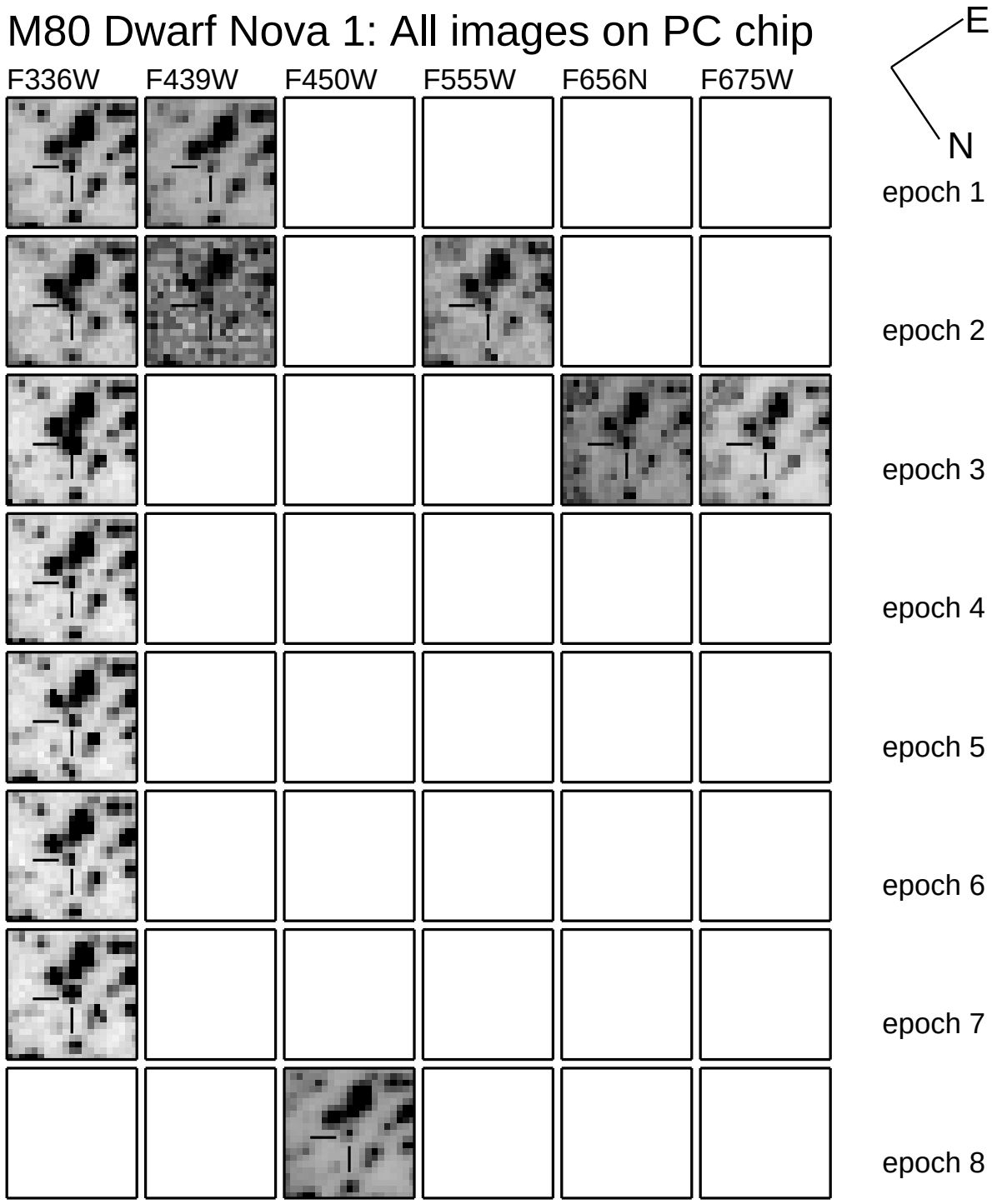

Fig. 6.— Thumbnail images for the first Dwarf Nova (DN1) in M80. It can clearly be seen in eruption in epoch 3. Each thumbnail is 1.04 arcseconds on a side, and North and East are indicated at the upper right.

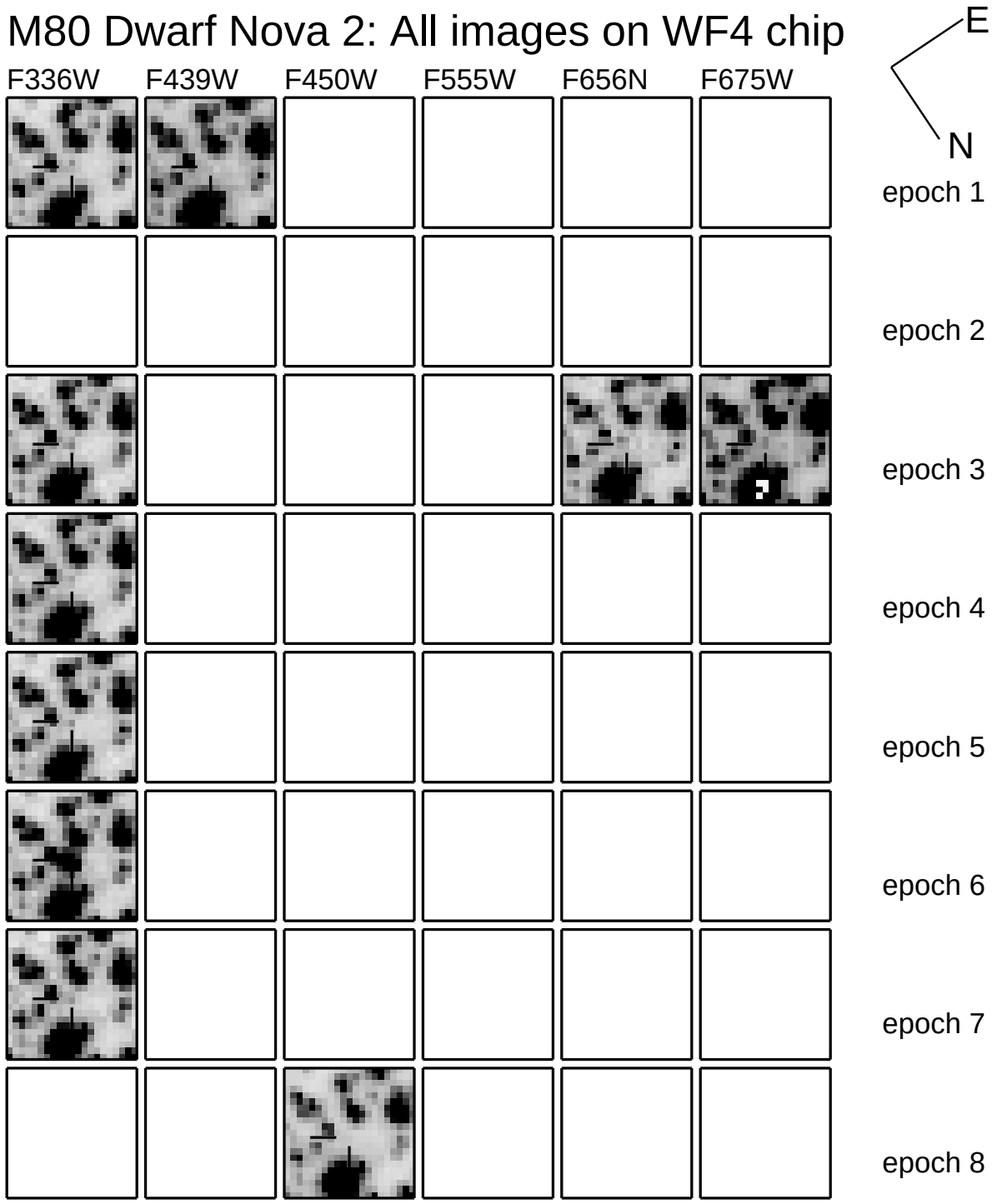

Fig. 7.— Thumbnail images for the second Dwarf Nova (DN2) in M80. It is in eruption in epoch 6 and just off the PC chip in epoch 2. Each thumbnail is 2.1 arcseconds on a side, and North and East are indicated at the upper right.

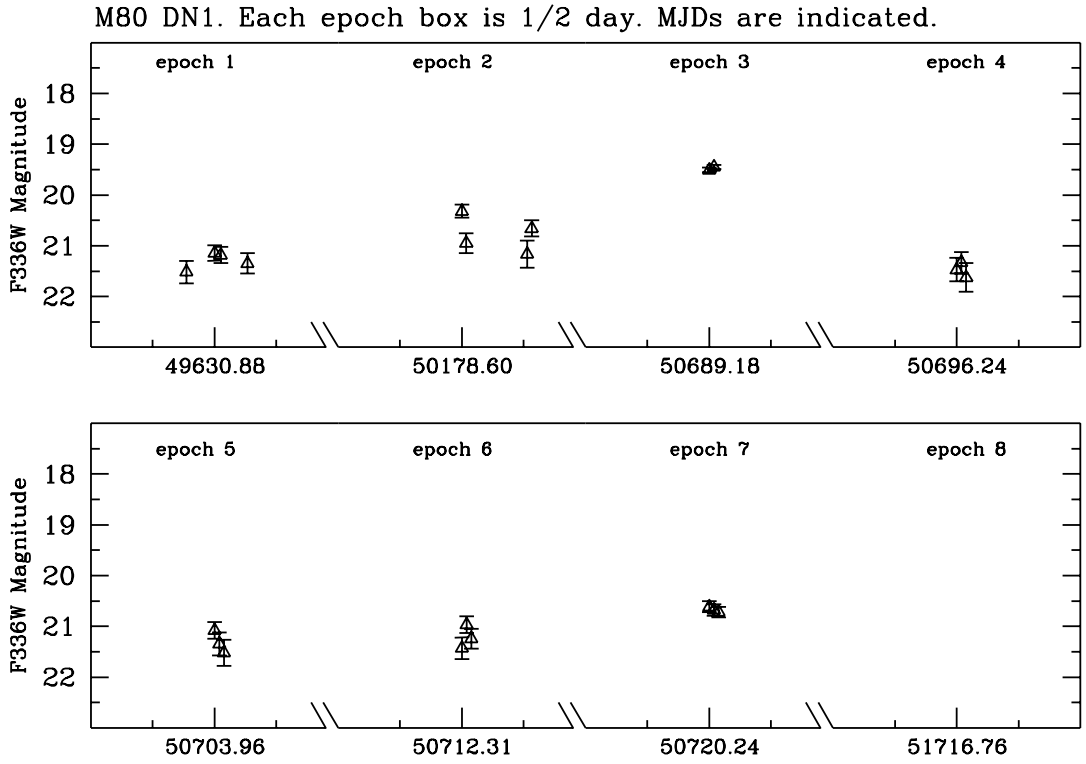

Fig. 8.— The lightcurve for the first Dwarf Nova (DN1) in F336W. The object is in eruption in epoch 3.

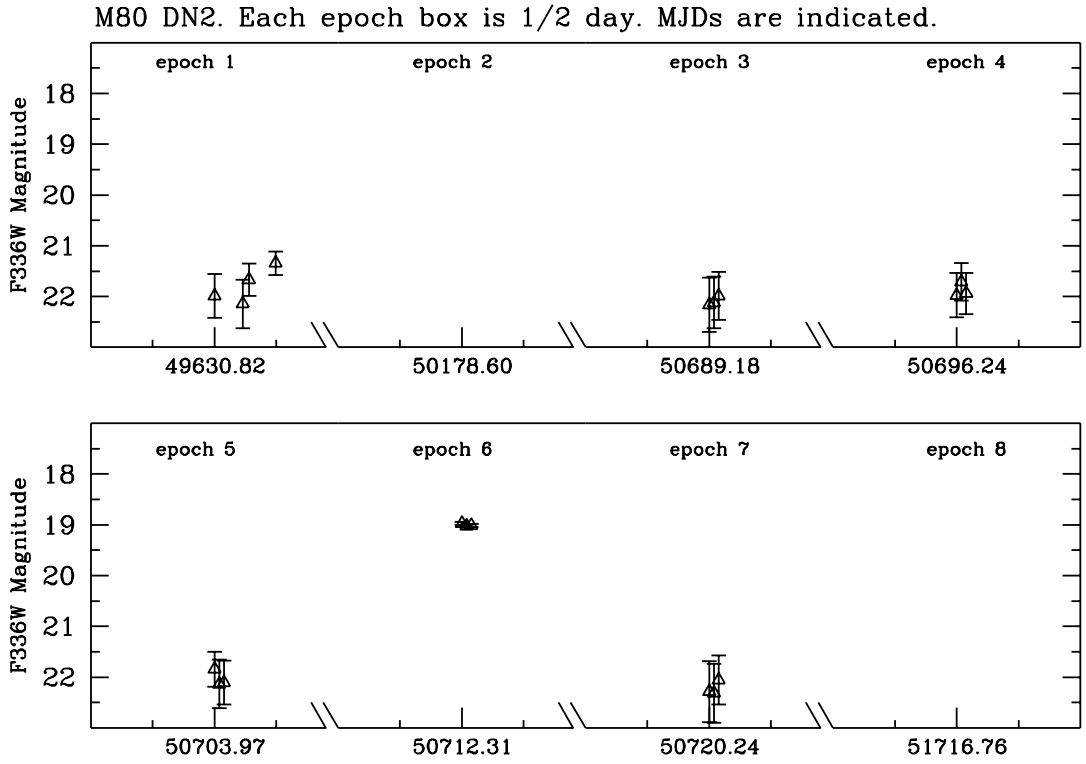

Fig. 9.— The lightcurve for the second Dwarf Nova (DN2) in F336W. The object is in eruption in epoch 6, and just outside the field-of-view in epoch 2.

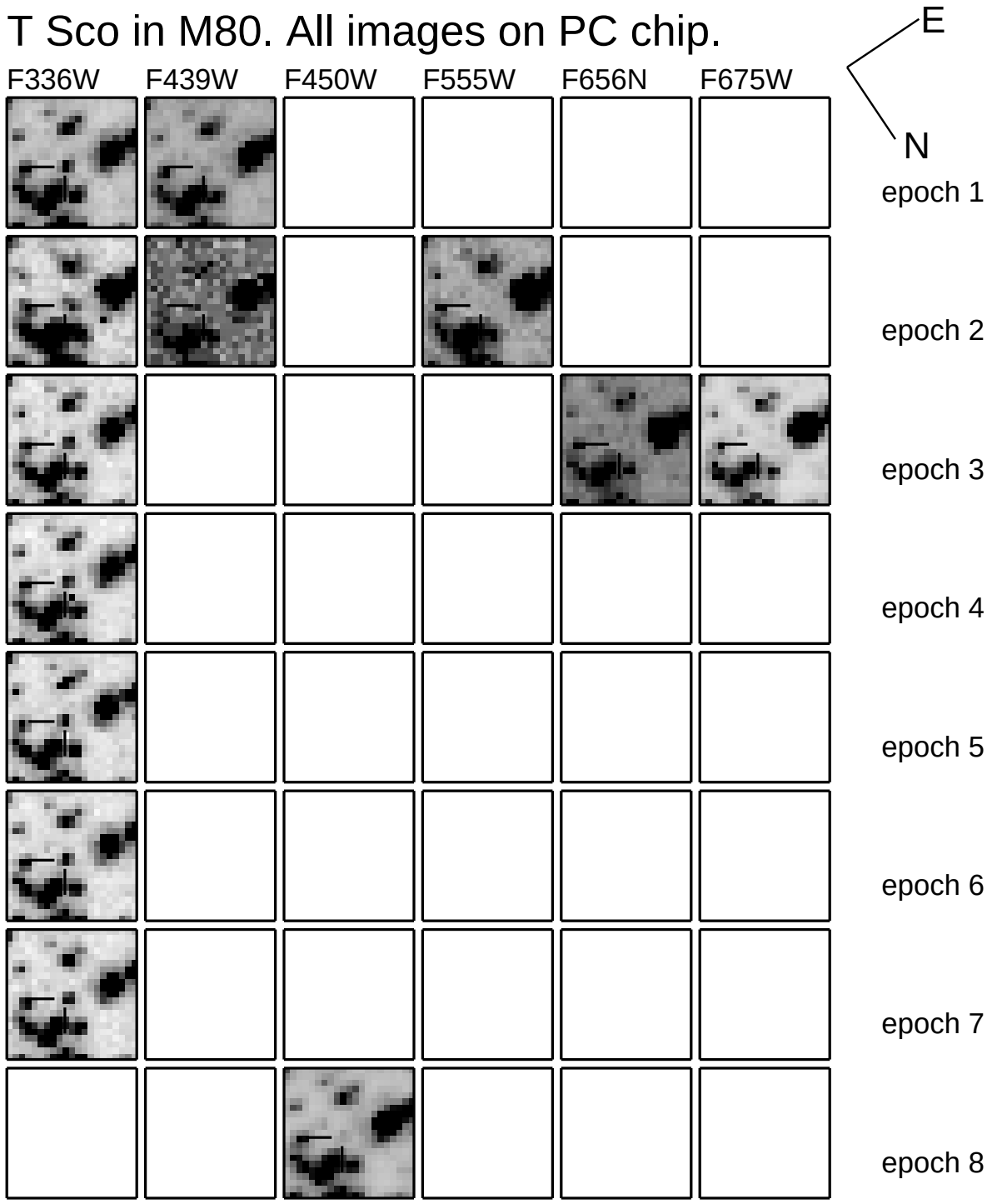

Fig. 10.— Thumbnail images of the classical nova T Sco in M80. These can be compared to Shara and Drissen (1995). Each thumbnail is 1.04 arcseconds on a side.

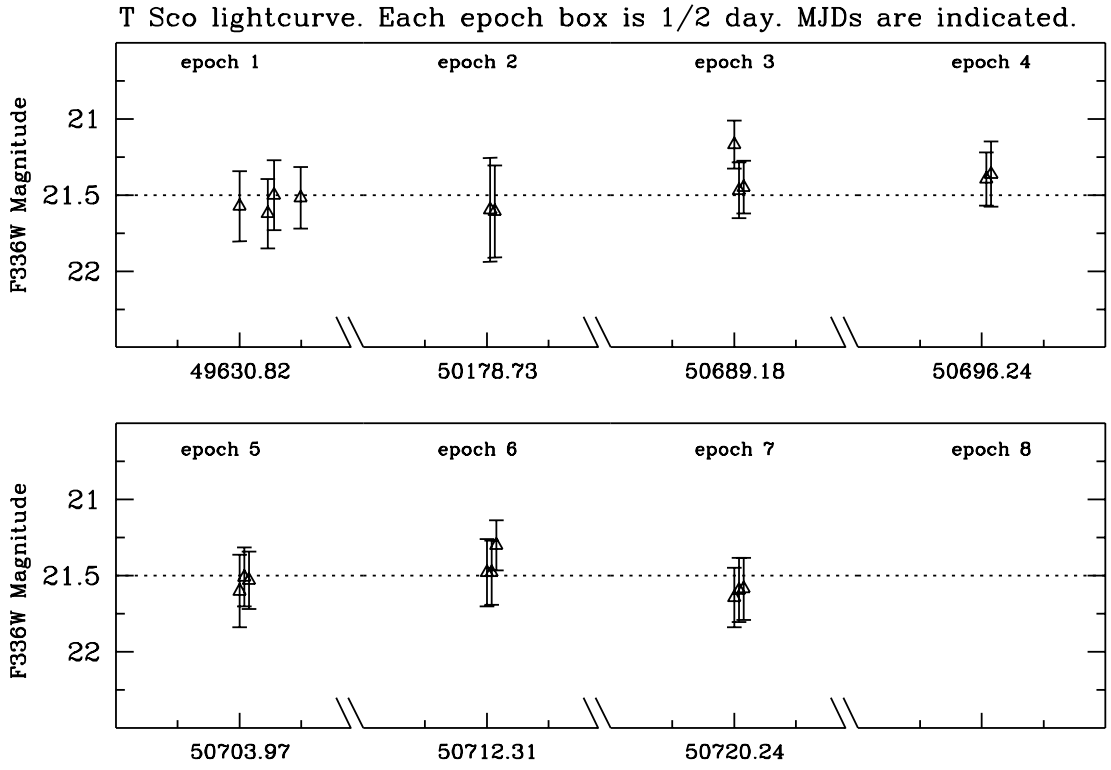

Fig. 11.— F336W Photometry for the old nova T Sco (nova 1860). The object is remarkably constant in brightness.

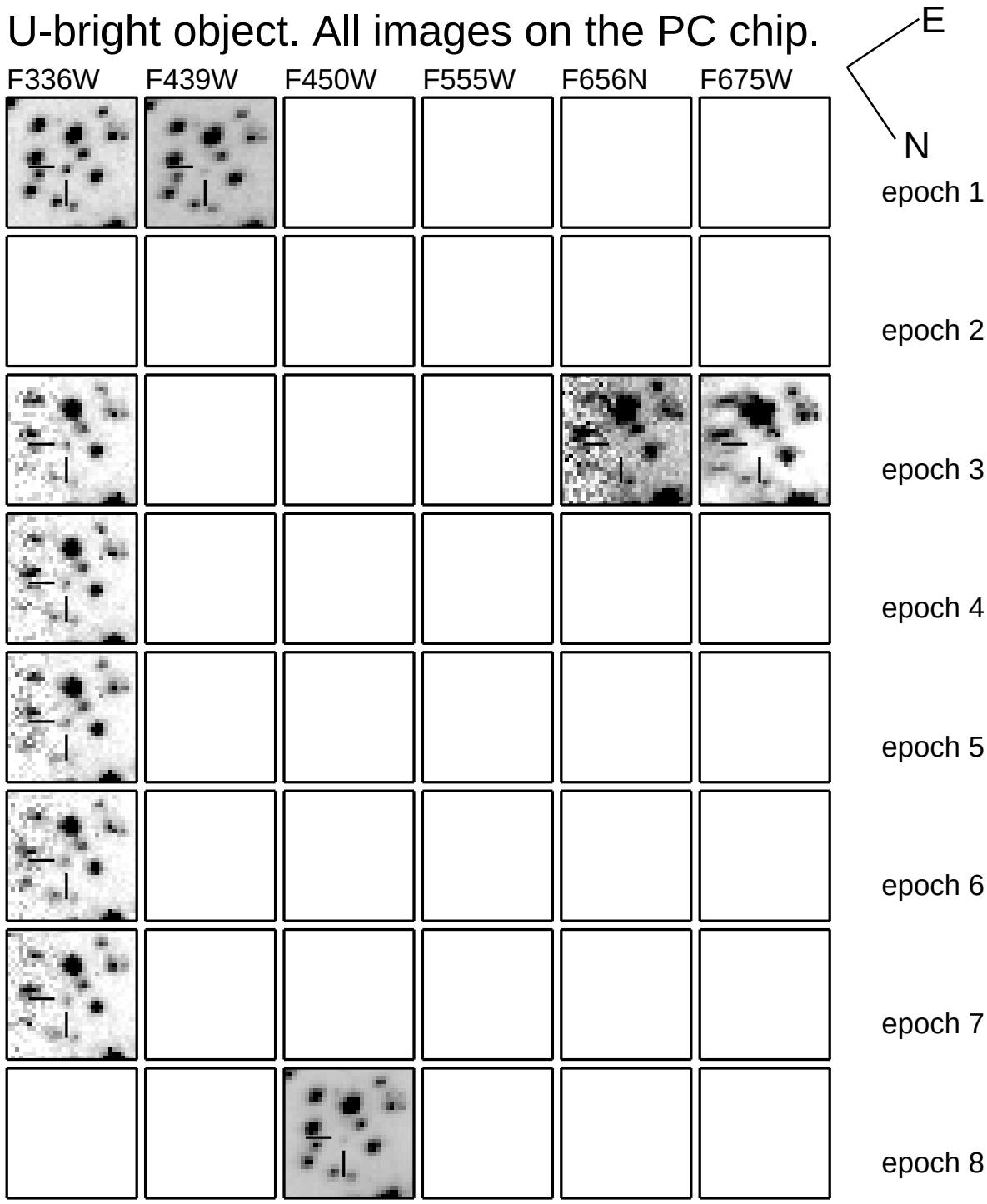

Fig. 12.— Images of the extremely Blue object of Shara & Drissen (1995). Note that for epochs 3-7, the object is near the edge of the PC chip. The object was just off the chip in epoch 2. Each thumbnail is 1.54 arcseconds on a side.

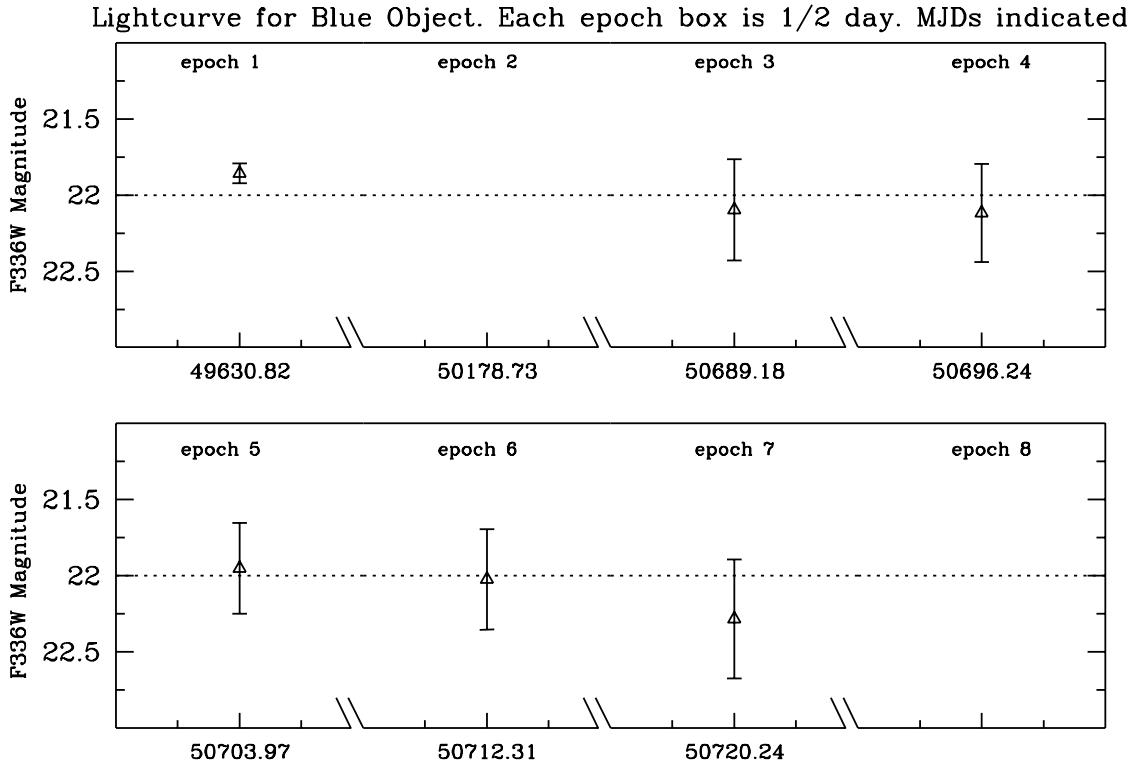

Fig. 13.— An F336W lightcurve for the faint blue object. The large error bars in epochs 3-7 are due to the relatively low S/N caused by the object's proximity to the chip edge.

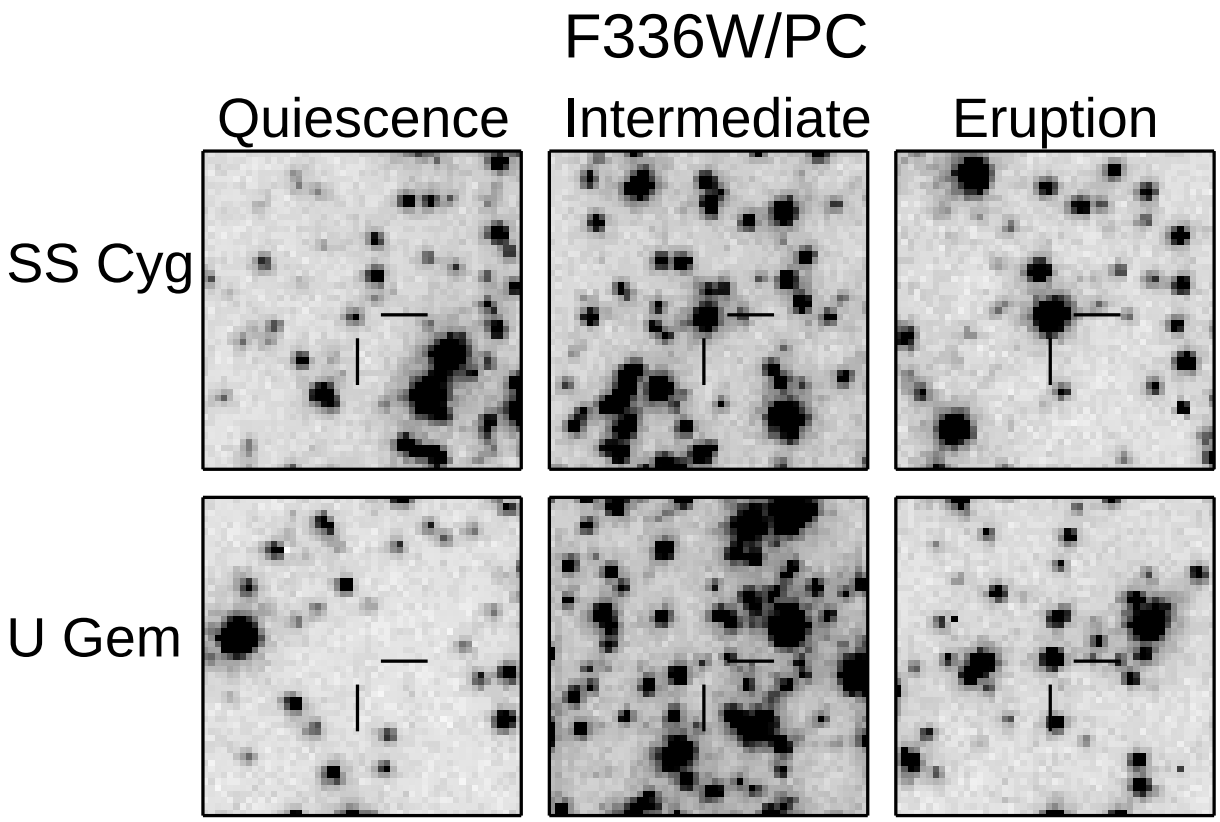

Fig. 14.— Examples of artificial Dwarf Novae in M80. Typical images of the two prototypical Dwarf Novae SS Cyg and U Gem, placed in M80 F336W PC images, are shown in three different phases, from quiescence to eruption.

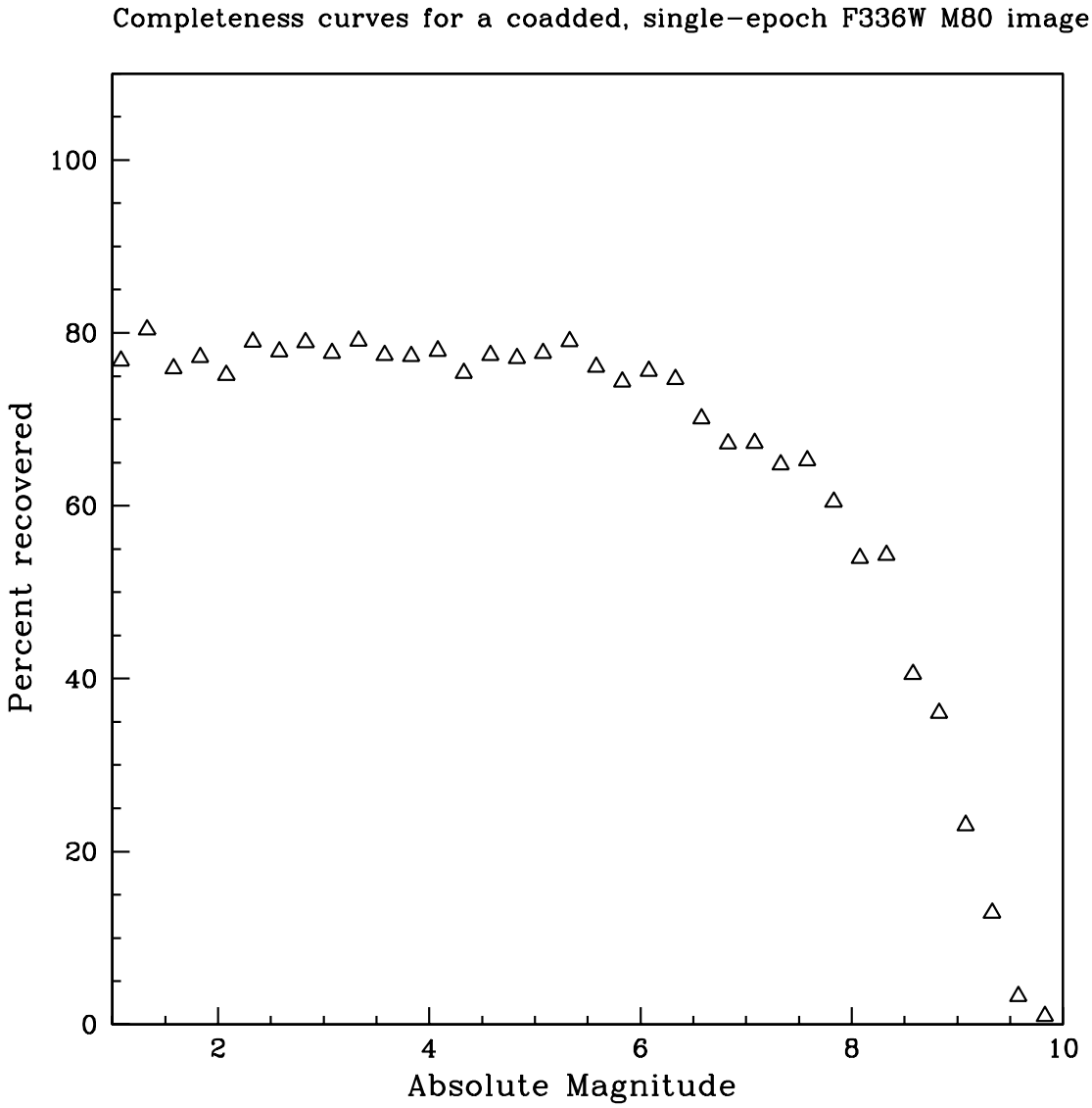

Fig. 15.— Completeness curves for a single-epoch coadded F336W image of M80. The figure assumes an M80 distance modulus of $(m - M) = 15.06$. Several hundred artificial stars were added to the F336W image in each magnitude bin. Only those stars recovered at the same position AND within 0.5 mag of the artificial star were considered recovered. Crowding accounts for the $\sim 20\%$ incompleteness for magnitudes between 0 and ~ 6.

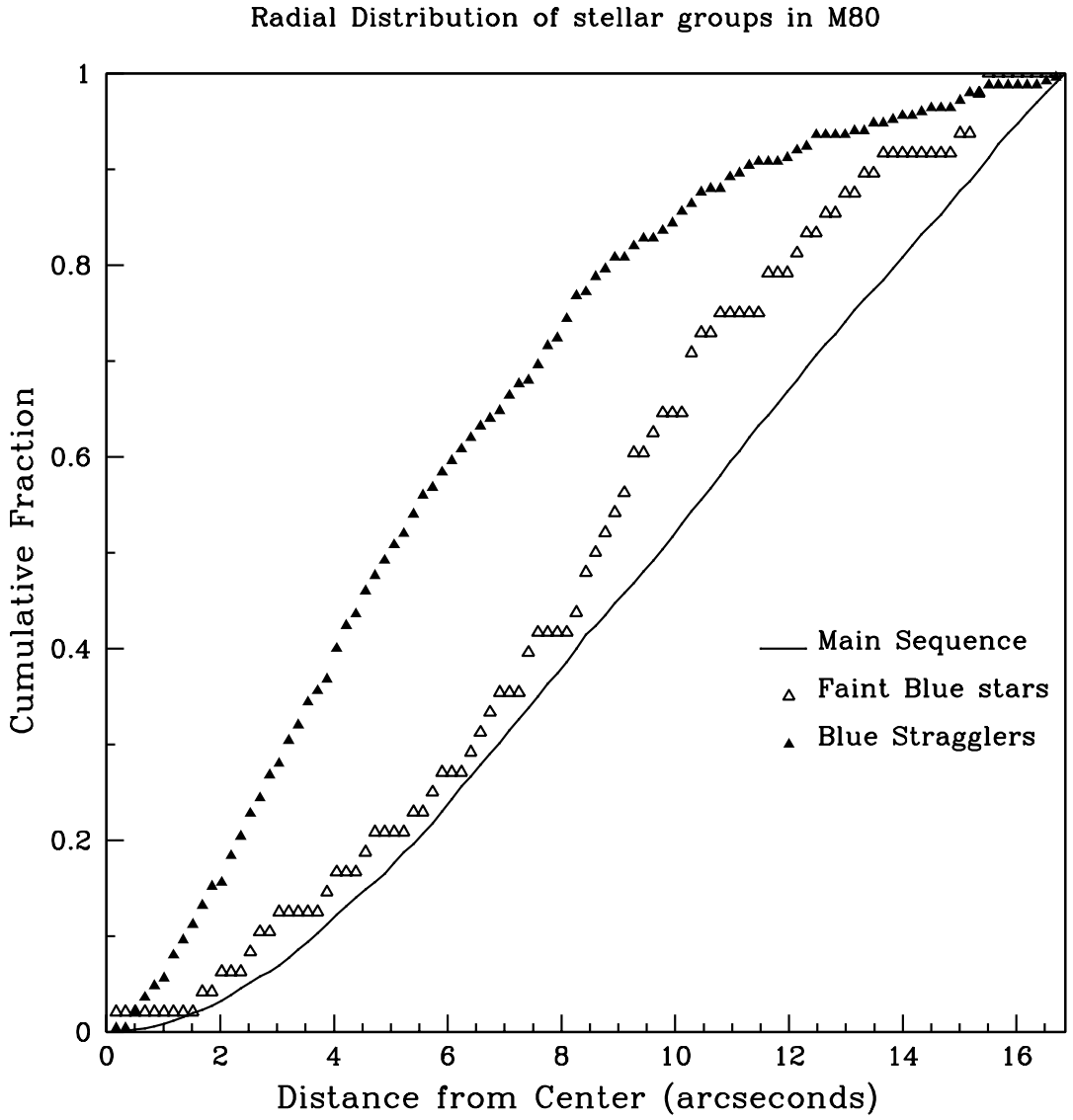

Fig. 16.— The cumulative radial distribution of three different groups of stars as indicated. The open triangles correspond to the faint blue stars running nearly parallel to the main sequence indicated in Figure 5. Their radial distribution differs from that of the main sequence stars (from the K-S test) with $> 95\%$ likelihood

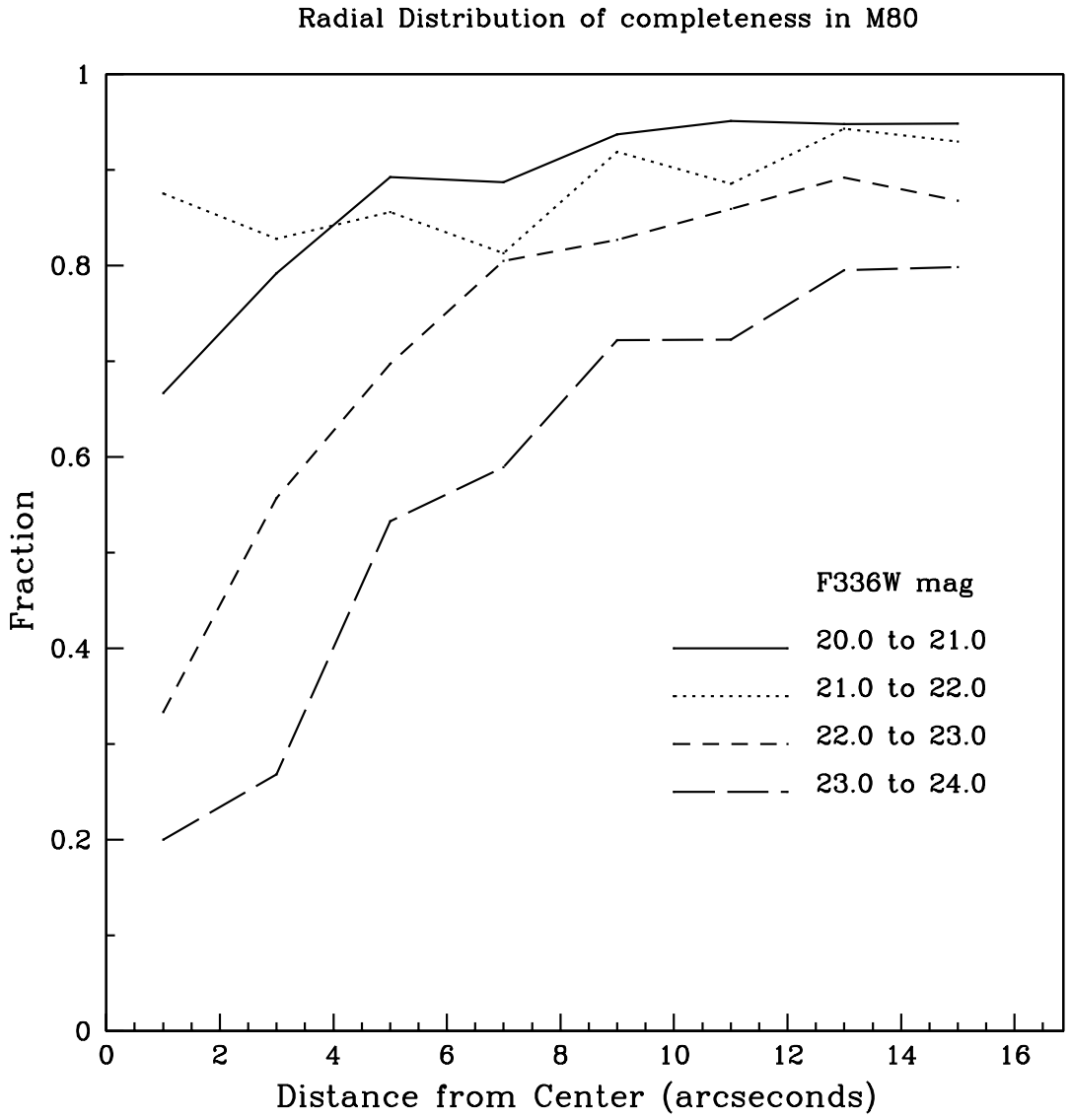

Fig. 17.— A simulation showing the recovery fraction of a sample of artificial stars randomly placed on an F336W image as a function of distance from the cluster center. We are significantly incomplete at $r < 8$ arcsec for stars fainter than $\simeq 22.0$ magnitude. This further strengthens the suggestion (From Figure 16) that the faint blue stars in M80 are centrally concentrated and hence good binary candidates.

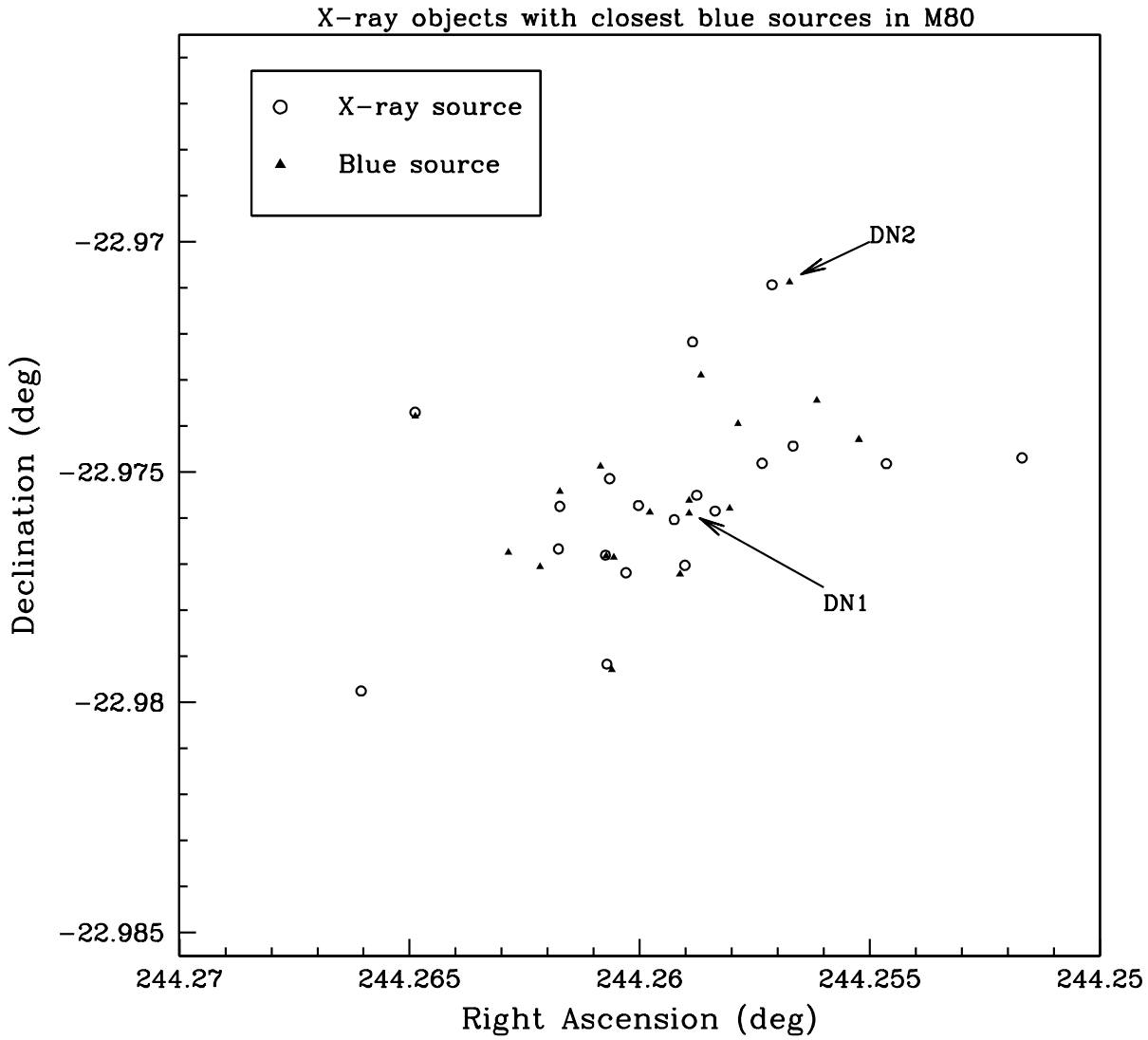

Fig. 18.— A plot showing the positions (circles) of the 19 X-ray bright sources noted by Heinke et al. (2003). The positions (triangles) of the closest faint blue stars are also shown (see text). The locations of Dwarf Nova 1 and 2 are marked.

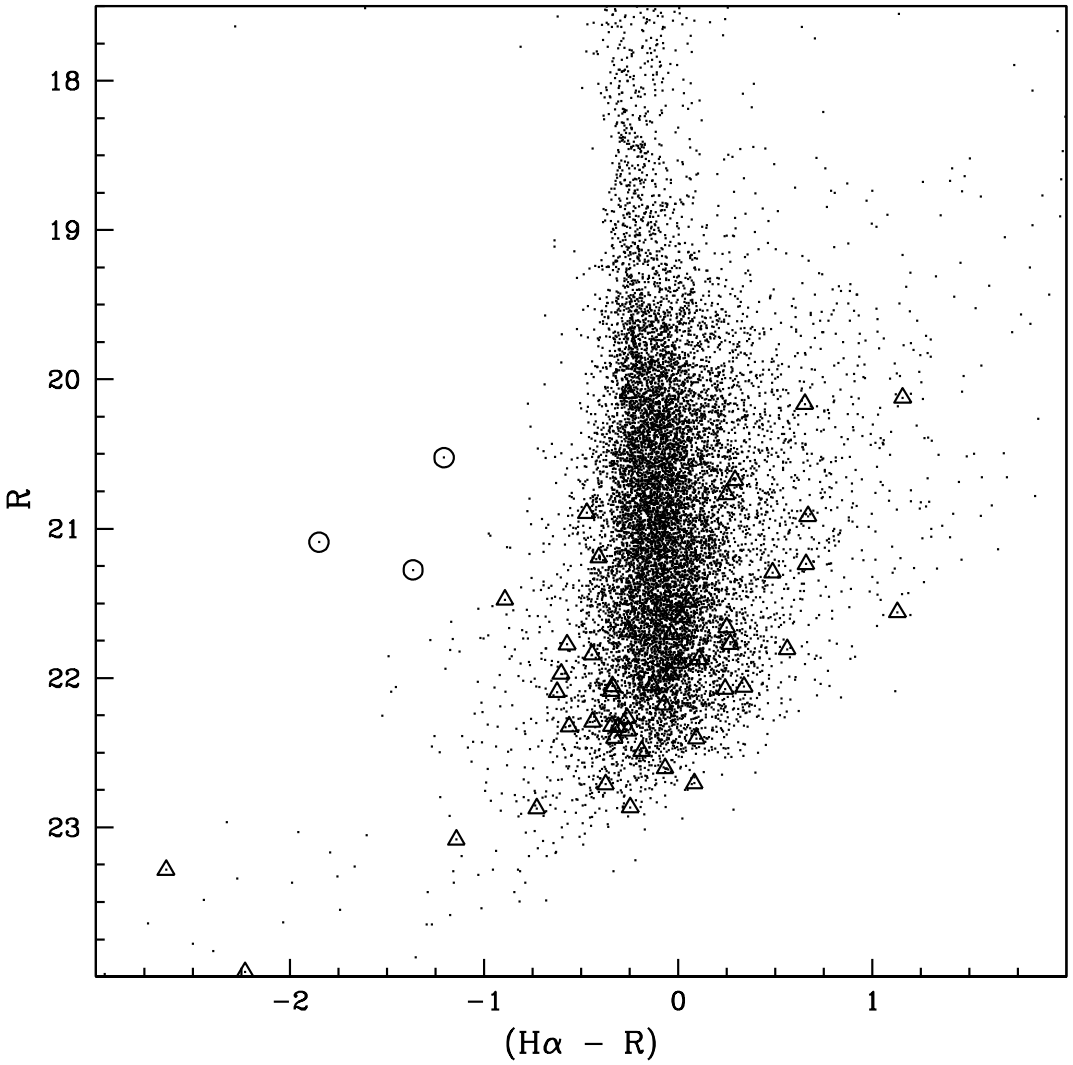

Fig. 19.— An R versus H$\alpha - R$ color-magnitude diagram with 51 of the faint blue objects (see Fig. 5) marked with triangles (see text). None of these faint blue objects appear to have an Hα luminosity significantly greater than the overall cluster population. The three circled objects are heavily crowded stars near the cluster core, and their photometry is thus highly suspect.

Table 1. Table of M80 observations: Listed are the number of useable observations at each date, as well as the total exposure time.

Epoch	PI/Prog. ID	F336W	F439W	F450W	F555W	F656N	F675W
1: 10/5/94	Shara #5677	4×900s ⇒3600s	4×300s ⇒1200s				
2: 4/5/96	Ferarro #5903	4×600s ⇒2400s	2×30s ⇒60s		2×2s, 4×23s ⇒96s		
3: 8/29/97	Shara #6460	2×700, 800s ⇒2200s				3×1300s ⇒3900s	3×260s ⇒780s
4: 9/5/97	Shara #6460	2×700, 800s ⇒2200s					
5: 9/12/97	Shara #6460	2×700, 800s ⇒2200s					
6: 9/21/97	Shara #6460	2×700, 800s ⇒2200s					
7: 9/29/97	Shara #6460	2×700, 800s ⇒2200s					
8: 6/21/00	King #8655			5×160s, 7× 200s ⇒2200s			

Table 2. List of the 19 bright X-ray sources from Heinke et al. (2003) with the closest blue objects, and their separation in arcseconds, after applying the offsets discussed in the text.

Source	R.A. (X-ray)	Decl. (X-ray)	R.A. (blue)	Decl. (blue)	Δ	Notes
CX1	16 17 02.814	-22 58 32.67	16 17 2.813	-22 58 31.51	1.160	
CX2	16 17 02.576	-22 58 36.48	16 17 2.573	-22 58 36.55	0.085	
CX3	16 17 01.597	-22 58 27.95	16 17 1.474	-22 58 24.38	3.969	
CX4	16 17 02.005	-22 58 33.03	16 17 1.928	-22 58 32.80	1.086	
CX5	16 17 01.708	-22 58 15.34	16 17 1.612	-22 58 15.13	1.282	DN2
CX6	16 17 03.569	-22 58 25.30	16 17 3.569	-22 58 25.61	0.302	
CX7	16 17 02.164	-22 58 37.27	16 17 2.189	-22 58 37.95	0.766	
CX8	16 17 01.114	-22 58 29.33	16 17 1.255	-22 58 27.44	2.731	
CX9	16 17 02.401	-22 58 32.60	16 17 2.346	-22 58 33.13	0.967	
CX10	16 17 00.407	-22 58 28.87	16 17 1.255	-22 58 27.44	11.820	
CX11	16 17 02.472	-22 58 37.86	16 17 2.532	-22 58 36.66	1.483	
CX12	16 17 02.565	-22 58 45.00	16 17 2.539	-22 58 45.44	0.564	
CX13	16 17 01.755	-22 58 29.29	16 17 1.880	-22 58 26.22	3.524	
CX14	16 17 02.553	-22 58 30.50	16 17 2.601	-22 58 29.53	1.176	
CX15	16 17 02.100	-22 58 31.80	16 17 2.141	-22 58 32.19	0.680	
CX16	16 17 02.119	-22 58 19.80	16 17 2.079	-22 58 22.40	2.666	
CX17	16 17 02.220	-22 58 33.70	16 17 2.141	-22 58 33.20	1.174	DN1
CX18	16 17 02.820	-22 58 36.00	16 17 2.916	-22 58 37.38	1.901	
CX19	16 17 03.850	-22 58 47.10	16 17 3.081	-22 58 36.26	15.172	